JOURNAL OF MATERIALS SCIENCE 28 (1993) 2260–2266

Crystal nucleation kinetics in a $40CaO–40P_2O_5–20B_2O_3$ glass – a study of heterogeneously catalysed crystallization

P. F. JAMES, W. SHI
Department of Engineering Materials, The University of Sheffield, Sir Robert Hadfield Building, Mappin Street, Sheffield S1 4DU, UK

The crystallization mechanism and nucleation kinetics in a $40CaO–40P_2O_5–20B_2O_3$ glass were studied using differential thermal analysis, X-ray diffraction, optical microscopy and scanning electron microscopy/energy dispersive analysis of X-rays. After heat treatments at temperatures around the glass transformation temperature, T_g, the first phase to precipitate was BPO_4 and subsequently the phase $4CaO \cdot P_2O_5$ appeared by heterogeneous nucleation on the BPO_4. The kinetics of nucleation were studied as a function of temperature. The maximum nucleation rate occurred at 620 °C, which is close to T_g. The crystallization peak height from differential thermal analysis was also used to determine the temperature of the maximum nucleation rate.

1. Introduction

Glass-ceramics, materials made by the controlled crystallization of glasses, have a wide range of applications. Their excellent mechanical, electrical and thermal properties depend on the fine-grain crystalline microstructures produced by high-volume nucleation in the parent glasses [1]. Most glass-ceramics are based on silicates and the kinetics of crystal nucleation have been intensively studied in silicate glasses [2, 3]. In contrast, there have been comparatively few studies of nucleation kinetics and of glass-ceramic formation in phosphate-based systems. Phosphate glass-ceramics have potential applications, for example, as biomedical or dental materials and as sealing materials to high thermal-expansion metals [4].

Volume or "bulk" nucleation is generally difficult to find in phosphate glasses and usually only surface nucleation is observed on heat treatment. James and Wang [5–7], however, found that additions of Al_2O_3 (typically around 7 mol %) were effective in promoting volume nucleation in $CaO–P_2O_5$ glasses. Heat treatment produced high-bulk nucleation of $AlPO_4$ crystals which acted as heterogeneous sites for crystallization of the major calcium phosphate phase. Fine-grain glass-ceramics prepared in this way possessed good machineability and biocompatibility [7]. Recently, Shi and James [8] in a study of the structure, properties and general crystallization behaviour of glasses with compositions $(50 - x/2)CaO–(50 - x/2)P_2O_5–xB_2O_3$ (x = 0–45 mol %), found that for B_2O_3 contents between 15 and 25 mol %, volume nucleation occurred. However, B_2O_3 was apparently not as effective a "nucleation agent" as Al_2O_3 for $CaO–P_2O_5$ glasses. Al_2O_3 addition resulted in much finer grain glass-ceramic materials [7].

In the present work, a detailed study of the nucleation kinetics in the composition $40CaO–40P_2O_5–20B_2O_3$ (mol %) is presented using quantitative measurements of crystal number densities from reflection optical micrographs. The temperature of the maximum nucleation rate was also determined using differential thermal analysis (DTA). The crystallization mechanism was investigated by X-ray diffraction (XRD), and scanning electron microscopy (SEM) in conjunction with energy dispersive X-ray analysis (EDAX). The objective was to explore the potential of B_2O_3 as a nucleating agent using a promising composition from the preliminary study [8]. However, the results are also of general interest as a study of the nucleation kinetics in a system in which the first phase to appear heterogeneously catalyses the crystallization of a major phase. There have been few, if any, such studies, whereas the nucleation kinetics in silicate systems, without deliberate addition of a nucleating agent, have been widely investigated [2]. In these systems homogeneous nucleation probably occurs.

2. Experimental procedure

A $40CaO–40P_2O_5–20B_2O_3$ (mol %) glass was prepared from reagent grade calcium hydrogen phosphate, $CaH_4(PO_4)_2 \cdot H_2O$, and boric acid, H_3BO_3. The mixed batch was sintered first at 700 °C and melted in an alumina crucible at 1250 °C for 2 h. The melt was then poured on to a preheated steel plate. The glass was not annealed in order to avoid the possibility of nucleation during the annealing treatment. Samples were given isothermal nucleation heat treatments in the range 575–650 °C in an accurately controlled tube furnace. The nucleation temperatures were chosen in a range around the glass transformation temperature (613 °C from DTA), following previous experience with silicate compositions [2]. Following nucleation, the samples were heat treated at

0022–2461

a higher growth temperature (770 °C) for a short time (usually 15 min) in a separate furnace to grow the nucleated crystals to dimensions observable in the optical microscope. The growth treatment (temperature and time) was chosen to avoid extensive overlapping of crystals. Also it was essential that the nucleation rate at the growth temperature was negligible compared with that in the first-stage treatment The assumptions of this method are discussed later.

After heat treatment, glass samples were mounted on glass slides with Canada balsam, ground flat to remove any surface crystallization, polished with cerirouge, and lightly etched for up to 45 s in a $2HF \cdot 2HCl \cdot 96H_2O$ (vol %) solution. Optical micrographs were then taken in reflection using a Polyvar optical microscope. The number of crystal particles (spherulites) per unit volume, N_v, was determined from the optical micrographs using the method of Dehoff and Rhines [9] for random plane sections through an ellipsoid. The method has been discussed in detail by James [10]. The crystal particles in the present glass after double-stage heat treatment were spherical, which simplified the analysis. The following equations were used for the calculation of the number density of spheres

$$N_v = \frac{2ZN_s}{\pi} \quad (1)$$

$$Z = \frac{\sum_i N_{si}/D_i}{\sum_i N_{si}} \quad (2)$$

The particles (spheres) were divided into groups according to their diameters, the sub-group i corresponding to an average diameter D_i; N_s the total number of particles per unit area; N_{si} the number of particles per unit area in the sub-group i; Z is the mean value of the reciprocals of the measured diameters over all possible circular intersections. For each heat treatment, measurements were made of the diameters of around 200 particle intersections in a known area of enlarged prints and N_v calculated. The 95% confidence limits on N_v values were approximately $\pm$ 15% from random sampling errors. Systematic errors in N_v arising from the resolution limit of detection in the optical microscope, recently analysed in detail by Zanotto and James [11], were negligible in the present experiments because the majority of the intersection diameters were large, typically ranging up to 100 μm.

Differential thermal analysis (DTA) was carried out using a Stanton Redcroft DTA-673 apparatus at a heating rate of 10 °C min^{-1}. The sample, in the form of 100 mg powder, and the calcined alumina reference material were contained in platinum crucibles. The method used for the determination of the temperature of the maximum nucleation rate by DTA is described later: it is based on the observation that the intensity at T_c (peak height) increases as the nucleation heat-treatment temperature approaches the temperature of maximum nucleation rate [12, 13].

The crystalline phases present after heat treatment were identified by a Philips X-ray diffractometer with CuK_α radiation.

3. Results and discussion

3.1. Nucleation and crystallization mechanism

After heat treatments in a range of temperatures around the glass transformation temperature, T_g, the glass showed volume nucleation and significant crystal growth occurred during the second stage of heat treatment. A typical reflection optical micrograph of crystalline spheres precipitated after two-stage heat treatment is shown in Fig. 1. The XRD spectra showed that the first precipitated phase to be detected in either single- or two-stage heat treatments was BPO_4, followed by the appearance of the $4CaO \cdot P_2O_5$ crystal phase (see Fig. 2). A list of measured d spacings for the two phases is given in Table I.

The crystal structure of BPO_4 is tetragonal with a, b values of 0.4338 and 0.6645 nm, respectively (JCPDS 14-696). The crystal structure of $4CaO \cdot P_2O_5$ is monoclinic with a, b, c values of 0.7018, 1.1980 and 0.9469 nm, respectively (JCPDS 25-1137).

When the crystalline spherulites were observed by SEM at higher magnification (Fig. 3), a distinct "core" region was observed in the centre of each spherulite. This suggests that the core regions are composed mainly of the phase BPO_4 and are surrounded by the $4CaO \cdot P_2O_5$ phase. To confirm this, SEM in conjunction with energy dispersive X-ray analysis was used to analyse the central core and outer regions of the spherulites. In the element analysis, phosphorus and calcium could be readily detected, but not boron because of the limitation of the EDAX technique (see Fig. 4a). In the central core phosphorus was a major constituent and there was a minor peak from calcium. In contrast to this, both calcium and phosphorus were detected as major elements in the fan-like or radial growth areas surrounding the central phase and the amount of calcium was significantly increased (see Fig. 4b). This is supporting evidence that the outer radial growths are of the phase $4CaO \cdot P_2O_5$. From the point of view of crystallography, the fairly close c parameter (0.6645 nm) of BPO_4 to the a parameter (0.7018 nm) of $4CaO \cdot P_2O_5$ may also support the proposed crystallization process of epitaxial growth of $4CaO \cdot P_2O_5$ on the BPO_4 phase. Fig. 5a shows the boundary of two impinging crystal spherulites and

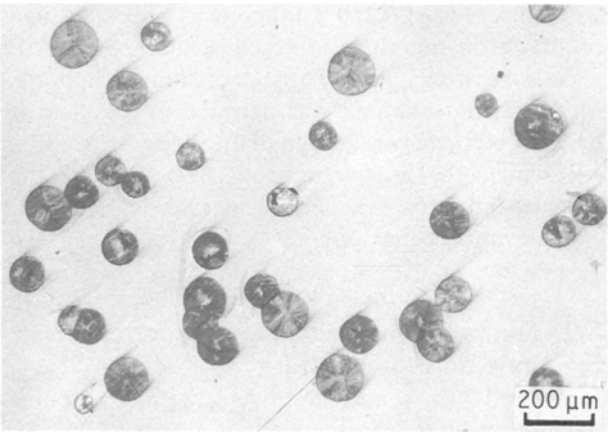

Figure 1 $40CaO–40P_2O_5–20B_2O_3$ glass nucleated at 620 °C for 0.5 h followed by 770 °C for 15 min. Optical reflection micrograph.

TABLE I Experimental d from Fig. 2 with indexing according to JCPDS files for BPO_4 (JCPDS 14-696) and $4CaO \cdot P_2O_5$ (JCPDS 25-1137) (BP, BPO_4; CP, $4CaO \cdot P_2O_5$)

Fig. 2a		Fig. 2b		Fig. 2c		Phases in JCPDS	
d (nm)	I	d (nm)	I	d (nm)	I	Phase	d (nm)
0.363	10	0.363	12	0.3632	100	BP	(0.3632)
				0.3195	21	CP	(0.3190)
				0.3058	28	CP, BP	(0.3053), (0.3067)
				0.2995	40	CP	(0.2995)
				0.2891	20	CP	(0.2895)
				0.2787	12	CP	(0.2789)
				0.2761	11	CP	(0.2763)
				0.2652	5	CP	(0.2649)
				0.2251	10	BP	(0.2254)
				0.2109	8	CP	(0.2109)

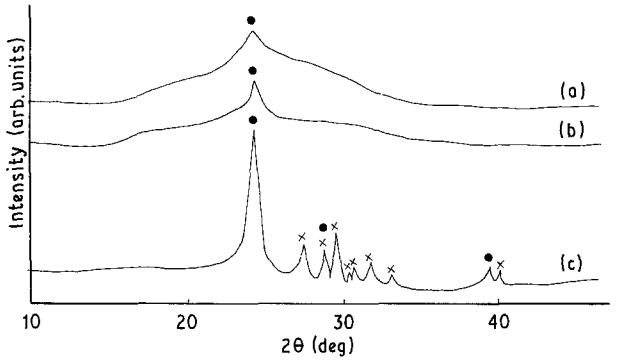

Figure 2 X-ray diffraction pattern of $40CaO–40P_2O_5–20B_2O_3$ glass heat treated at (a) 680 °C for 10 h; (b) 712 °C for 10 h and (c) 712 °C for 20 h. (●) Peaks corresponding to BPO_4, (×) $4CaO \cdot P_2O_5$ peaks.

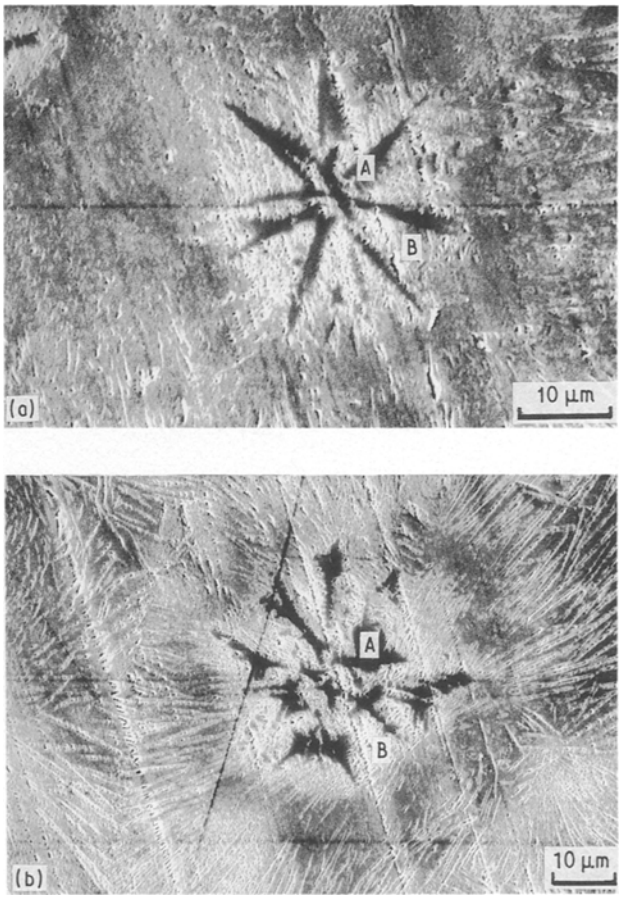

Figure 3 (a, b) Scanning electron micrographs showing higher magnification of part of the central region of crystal spherulites as shown in Fig. 1, in the glass nucleated at 600 °C for 10 h followed by 770 °C for 15 min. Region A is BPO_4 phase. Region B is $4CaO \cdot P_2O_5$ phase.

Fig. 5b illustrates the radial growth of the $4CaO \cdot P_2O_5$ phase at higher magnification. These micrographs appear to show a significant proportion of residual glass phase. This was also indicated by the translucent appearance of the samples after heat treatment.

The possible effects of alumina impurity in the glass on the crystallization behaviour should be considered, because the glass was melted in an alumina crucible and in view of previous results [5–7] that additions of around 7 mol % Al_2O_3 resulted in catalysed nucleation on $AlPO_4$ crystals. However, for the melting temperature used (1250 °C) there was no visible signs of attack on the alumina crucible after pouring the glass, suggesting minimal uptake of alumina impurity. Moreover, no alumina was detected in the glass by EDAX and there was no sign of the phase $AlPO_4$ from XRD after the heat treatments. We conclude that alumina impurity was insufficient to influence the crystallization behaviour.

3.2. Nucleation densities as a function of time and temperature

Figs 6 and 7 show nucleation densities, N_v, as a function of time after heat treatment at different first-stage (nucleation) temperatures. The same second-stage (growth) treatment at 770 °C for 15 min was used throughout. The nucleation densities increased with time at a given nucleation temperature. At lower temperatures (575, 590 and 600 °C), non-linear behaviour was observed at shorter times followed by linear behaviour at longer times. This can be attributed to non-steady-state nucleation, the nucleation rate (given by the slope of the N_v versus time plots) gradually approaching a constant equilibrium or steady state value, the process being characterized by an induction period. With increase in nucleation temperature the

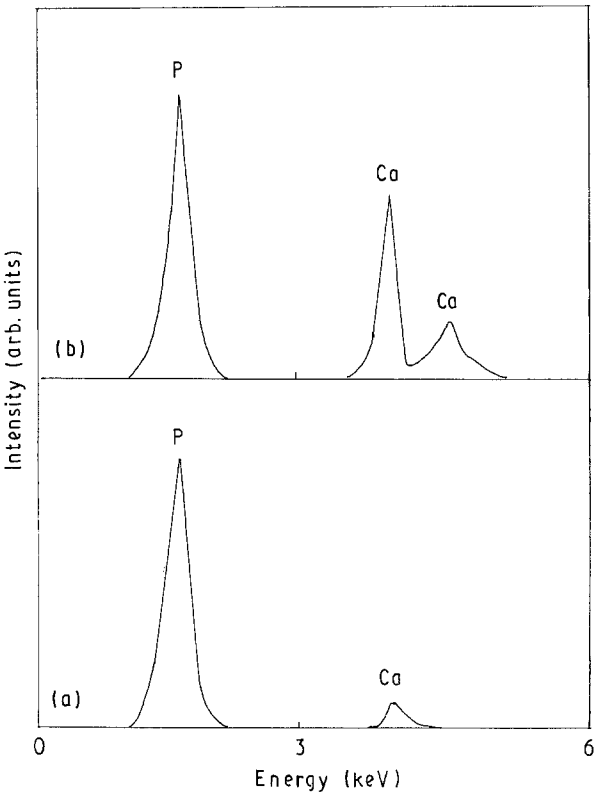

Figure 4 EDAX spectra showing the different compositions (a) at the centre of a spherulite corresponding to BPO_4 composition and (b) region of the crystal phase $4CaO \cdot P_2O_5$ shown in Fig. 3.

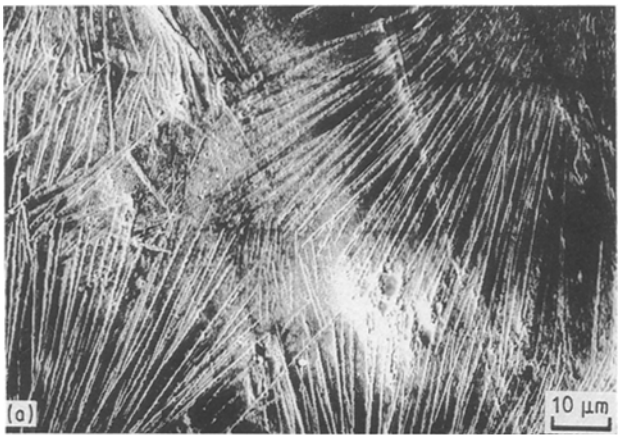

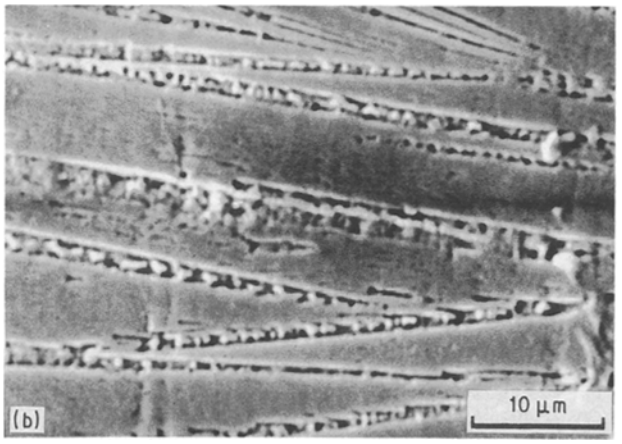

Figure 5 Scanning electron micrographs showing the morphology of $4CaO \cdot P_2O_5$ crystals (outer part of spherulites shown in Fig. 1) grown at 770 °C for 15 min after nucleation at 590 °C for 16.5 h. (a) Intersection of several crystals, (b) enlarged radial well-developed crystals.

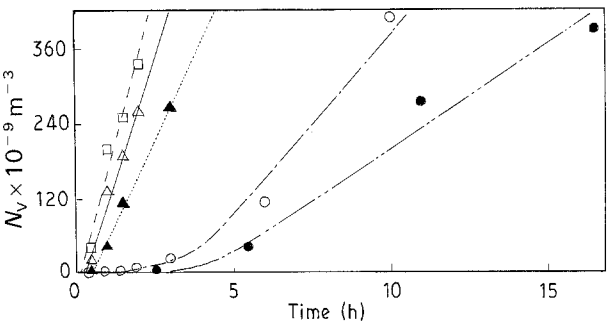

Figure 6 Crystal density, N_v, versus nucleation time for samples heated at different nucleation temperatures followed by growth at 770 °C for 15 min in the $40CaO-40P_2O_5-20B_2O_3$ glass. Nucleation temperatures: (●) 590 °C, (○) 600 °C, (△) 610 °C, (□) 620 °C and (▲) 630 °C.

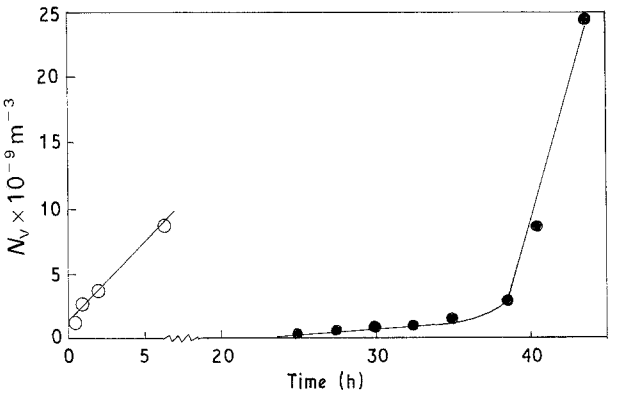

Figure 7 Crystal density, N_v, versus nucleation time for samples heated at different nucleation temperatures followed by growth at 770 °C for 15 min in the $40CaO-40P_2O_5-20B_2O_3$ glass. Nucleation temperatures: (●) 575 °C, (○) 650 °C.

induction time, as determined from the intercept on the time axis of a line through the points at longer times, decreased and eventually became so short that the plots of nucleation densities against time were practically linear through the origin, as shown in Figs 6 and 7 at higher temperatures (610, 620, 630 and 650 °C). The steady-state nucleation rate, I, was determined from the slope of the straight line drawn through the points at longer times, after the induction period was completed, using a least squares fit. Table II summarizes the results for I and the intercept (induction) time, t_A, at different nucleation temperatures.

The steady-state nucleation rate is plotted against temperature in Fig. 8. The $40CaO-40P_2O_5-20B_2O_3$ glass showed a maximum nucleation rate at about 620 °C. This temperature is quite close to the glass transformation temperature, T_g, from DTA which was 613 °C. It seems that detectable nucleation is observed only in the neighbourhood of the glass transformation temperature.

The non-steady-state nucleation behaviour observed at lower temperatures in the present glass is similar to that found in silicate systems [10, 14]. The steady-state nucleation rate in a supercooled liquid or glass is not achieved immediately at a constant temperature because an equilibrium size distribution of crystal "embryos" or clusters of the new phase is not

TABLE II Values of steady-state nucleation rate, I, and intercept time, t_A, at different nucleation temperatures

Temperature (°C)	t_A (min)	$I \times (10^{-7}\ m^{-3}\ s^{-1})$
575	2250	0.13
590	240	0.82
600	187	1.56
610	18	4.33
620	–	5.20
630	–	2.99
650	–	0.036

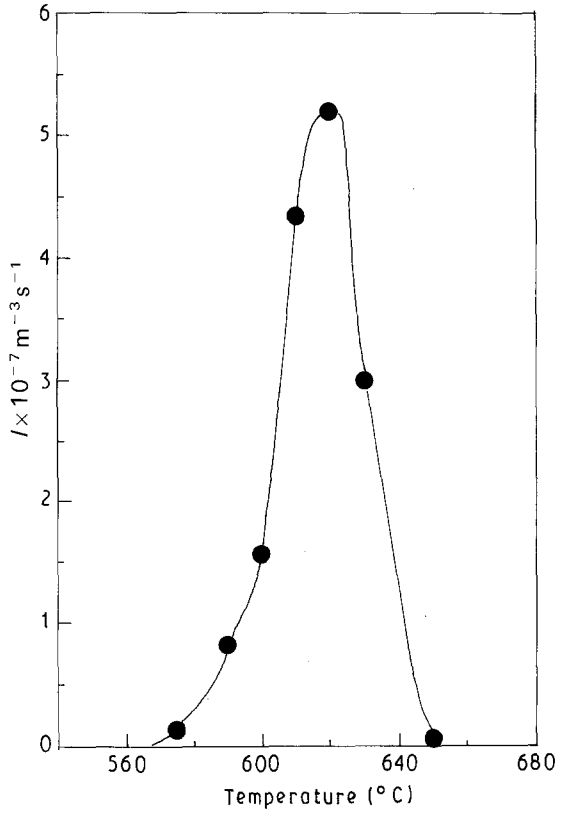

Figure 8 Steady-state nucleation rate versus nucleation temperature in $40CaO-40P_2O_5-20B_2O_3$ glass.

initially present, and takes time to develop. The induction time is a measure of the rate of approach to steady-state conditions. The N_v against time curves predicted by the equation of Kashchiev [15] for non-steady-state homogeneous nucleation in an undercooled liquid are found to describe well the experimental results in lithium disilicate glass [10]. The same theoretical curves also agree qualitatively with the shape of the N_v curves at lower temperatures (Figs 6 and 7) in the present phosphate system. However, it should be noted that two phases of different compositions occurred in the present glass after two-stage treatment. The simplest interpretation of the present results is that homogeneous nucleation of BPO_4 occurs during the first-stage heat treatment. The second-phase $4CaO \cdot P_2O_5$ appears probably by heterogeneous nucleation on the BPO_4 at a later time during either the first- or second-stage heat treatments. Thus it is the homogeneous nucleation of BPO_4 that determines the non-steady-state effects at lower temperatures.

The above results were obtained with the two-stage heat-treatment method, and it is appropriate to consider briefly its validity. The method is based on the assumptions that (a) after nucleation the glass contains an assembly of nuclei some of which will have grown into small crystals, the large majority of which do not redissolve on heating to the second stage; and (b) the nucleation rate at the growth temperature is negligible. Considering the first assumption, the size of the critical nucleus increases with rise in temperature according to classical theory. Consequently, a cluster of critical size at the lower temperature will not constitute a critical nucleus at the growth temperature and will tend to redissolve. However, during the nucleation stage, many of the nuclei that reach critical size will continue to grow and will attain a size larger than the corresponding critical size at the growth temperature. During the second growth stage, these nuclei will grow to observable dimensions. On this basis the number of particles observed after the growth stage should be close to the number of nuclei formed in the first-stage nucleation treatment. Assumption (a) was investigated experimentally for some silicate glasses [10, 14] and shown to be valid for a suitable choice of growth temperature. To minimize dissolution effects, the separation between the growth, T_G, and nucleation temperature, T_N, should be as low as possible, consistent with a reasonable growth rate, and negligible nucleation rate at T_G.

It was shown [14] that nucleus redissolution may cause a reduction in the measured N_v particularly for high values of the growth (second stage) temperature; and this can given an apparently higher value of the intercept (induction) time. The result is that the apparent ("total") intercept time t_A is the sum of the true intercept time due to non-steady-state nucleation, t_0, and the time, t_1, at the nucleation temperature, T_N, for nuclei to grow to sizes greater than critical size at the growth temperature, T_G. For homogeneous nucleation in lithium disilicate glass, using typical values of $T_N = 430\,°C$ and $T_G = 560\,°C$, t_1 was found experimentally to be about 10% of t_A. The dissolution effect caused a shift of the whole N_v versus t curve parallel to the time axis by an amount t_1. However, the steady-state nucleation rate determined from the slope of the plot at longer times was not affected. Similar effects are also expected in the present phosphate glass and it is reasonable to assume that non-steady-state nucleation rather than "dissolution" effects are the main cause of the observed intercept times.

3.3. Differential thermal analysis

Recently, the determination of the temperature of maximum nucleation rate by DTA methods has received considerable attention. The DTA technique is generally less time consuming than the traditional direct method involving the analysis of reflection micrographs, but the various methods of analysis used must be treated with caution in view of the assumptions generally employed. One method is based on

an analysis indicating that the inverse of the temperature, T_c, corresponding to the peak in the DTA crystallization exotherm will increase monotonically as the number density of nucleated particles increases [16]. Another method is based on the observation that the intensity at T_c (peak height) increases as the nucleation treatment temperature approaches the temperature of maximum nucleation rate [12]. Both methods are based on two assumptions. First it is assumed that all nucleation is completed prior to crystal growth, and secondly it is assumed that only one transformation mechanism occurs, namely, homogeneous crystal nucleation. Weinberg [13] recently demonstrated for two standard crystal-growth mechanisms, normal and screw dislocation growth, that T_c^{-1} will increase with the number density of nuclei in most systems. Most of the work so far has been applied to the $Li_2O \cdot 2SiO_2$ glass system because detailed nucleation and crystallization kinetics have been fully investigated in this system [10]. There are few publications available so far applying the DTA method to the determination of the maximum crystal nucleation rate temperature in other glass systems partly due to the uncertainties inherent in the DTA methods. In addition, the absolute values of crystal nucleation rates cannot be calculated simply from DTA traces.

In this work, differential thermal analysis (DTA) was applied to attempt to determine the nucleation rate curve for the $40CaO–40P_2O_5–20B_2O_3$ glass in which the crystal nucleation and crystallization mechanism had been investigated using the traditional method. The technique used here is slightly different from the published methods [12, 16] in which the nucleation heat treatment was carried out only in the DTA furnace. In this work, first it was confirmed that the quenched melt was glass by X-ray diffraction. Then small bulk samples were nucleated separately at different temperatures for the same time (0.5 h) in a tube furnace. The bulk samples were ground to remove surface layers and were finally ground to powder between 90 and 150 μm in size prior to a normal constant heating rate DTA experiment. It is assumed that the increase in DTA peak height is the direct result of an increasing concentration of nuclei in the glass. Consequently, the height of the DTA crystallization peak, which should be proportional to the concentration of nuclei in the glass, is expected to have a typical "bell" shape when plotted as a function of nucleation temperature. Fig. 9 shows the DTA crystallization peak height plotted against nucleation temperature. A maximum peak height around 620 °C was obtained. The shape of the curve is similar to that of Fig. 8 for the nucleation rate as determined by the more time consuming standard method. It is obvious that the simple DTA method used here provides a rapid way of determining the temperature corresponding to maximum nucleation for this glass. Ray and Day [12] have observed for $Li_2O \cdot 2SiO_2$ glass that the increase of crystallization peak height in $Li_2O \cdot 2SiO_2$ glass was accompanied by a decrease in T_c. However, this was not observed in the present $40CaO–40P_2O_5–20B_2O_3$ composition. It is suggested that although DTA methods are attractive and useful,

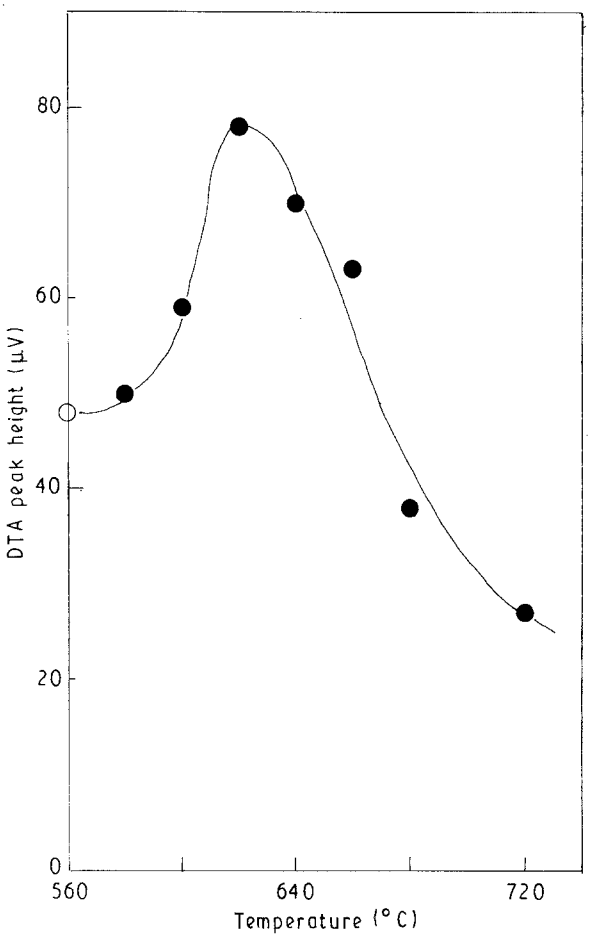

Figure 9 DTA peak height versus nucleation temperature (0.5 h) in $40CaO–40P_2O_5–20B_2O_3$ glass. (○) Peak height for glass with no nucleation treatment prior to DTA run.

it is advisable to check the results against the standard method wherever possible, because of uncertainties which may arise from factors such as the mechanism of nucleation (volume or surface) and the presence of steady-state or non-steady-state nucleation.

Although volume nucleation could be achieved in the $CaO–P_2O_5–B_2O_3$ system, nucleation rates were low and high-strength glass-ceramics could not be obtained after two-stage nucleation and growth heat treatments. However, further additions of alumina have been found to promote higher nucleation rates and fine-grain glass-ceramic formation in this system. These results will be discussed in a later paper.

4. Conclusions

The crystallization mechanism and kinetics of nucleation in the $40CaO–40P_2O_5–20B_2O_3$ (mol %) glass were studied by XRD, DTA, optical microscopy and SEM in conjunction with EDAX. It was found that volume crystal nucleation occurred after heat treatments around the glass transformation temperature, T_g. The first phase to precipitate on heat treatment was BPO_4 and subsequently the phase $4CaO \cdot P_2O_5$ appeared by heterogeneous nucleation on the BPO_4. The nucleation kinetics were determined by optical microscopy of samples given two-stage nucleation and growth heat treatments. For lower nucleation temperatures, non-linear behaviour between crystal number

density, N_v, and nucleation time, t, was observed at short times indicating non-steady-state nucleation. Linear behaviour of N_v versus t occurred at longer times, the nucleation rate reaching a nearly constant equilibrium or steady-state value after a certain induction period. With increase in nucleation temperature the induction time decreased and eventually became so short that the plots of nucleation densities against time were practically linear through the origin. The maximum nucleation rate occurred at 620 °C, which is close to T_g. The crystallization peak height from DTA was also successfully used to determine the temperature of maximum nucleation rate.

Acknowledgements

W. Shi wishes to thank the Chinese State Education Committee and the British Council for financial support.

References

1. P. W. McMILLAN, "Glass-Ceramics", 2nd Edn (Academic Press, London, 1979).
2. P. F. JAMES, in "Glasses and Glass Ceramics", edited by M. H. Lewis (Chapman and Hall, London, 1989) pp. 59–105.
3. P. F. JAMES and R. W. JONES, in "High Performance Glasses", edited by M. Cable and J. M. Parker, (Blackie, Glasgow, 1992) p. 102–32.
4. J. A. WILDER, Jr, J. T. HEALEY and B. C. BUNKER, in "Advances in Ceramics", Vol. 4, edited by J. H. Simmons, D. R. Uhlmann and G. H. Beall (American Ceramic Society, Columbus, OH, 1982), pp. 313–33.
5. P. F. JAMES, Brit. Pat. GB 2199028 (1986).
6. T. H. WANG, PhD thesis, The University of Sheffield (1987).
7. T. H. WANG and P. F. JAMES, in 'New Materials and their Applications", edited by D. Holland, Insititute of Physics Conference Series no. 111 (Institute of Physics, London, 1990) p. 401.
8. W. SHI and P. F. JAMES, *J. Mater. Sci.* **28** (1993) 469.
9. R. T. DEHOFF and F. N. RHINES, *Trans. Metall. Soc. AIME*, **221** (1961) 975.
10. P. F. JAMES, *Phys. Chem. Glasses* **15** (1974) 95.
11. E. D. ZANOTTO and P. F. JAMES, *J. Non-Crystalline Solids* **124** (1990) 86.
12. C. S. RAY and D. E. DAY, *J. Amer. Ceram. Soc.* **73** (1990) 439.
13. M. C. WEINBERG, *ibid.* **74** (1991) 1905.
14. P. F. JAMES, in "Advances in Ceramics", Vol. 4, edited by J. H. Simmons, D. R. Uhlmann and G. H. Beall (American Ceramic Society, Columbus, OH, 1982) pp. 1–48.
15. D. KASHCHIEV, *Surf. Sci.* **14** (1969) 209.
16. A. MAROTTA, A. BURI and F. BRANDA, *J. Mater. Sci.* **16** (1981) 341.

Received 21 July
and accepted 2 September 1992